Report on developed models and control schemes for heat pump and storage integration in local communities

Pavani Ponnaganti
Birgitte Bak-Jensen
Jayakrishnan R Pillai
Pierre Vogler-Finck

AALBORG UNIVERSITY
DENMARK

Task 2.2: Modelling and control algorithms for smart integration of flexible heat units and storages, both on individual household and at community scale (Task leader: AAU-DET, Participants: NGD, SMU, SNT, Duration M6-M18)

In this task, smart models of (hybrid) heat pumps and thermal storage systems are created that can be used to optimize the energy consumption in individual households, community buildings and district heating networks. For the latter, the thermal units have to be intelligently coordinated in an optimal manner to utilize electricity during periods of low price and high renewable electricity production from renewable energy sources like wind and solar PV. In this task, large booster heat pumps in conjunction with district heating networks are used. Here the heat pumps boost the temperature of the water for the district heating, resulting in better energy efficiency and an increased local use of renewable energy sources. Models of the heat demand and heat storage potential of houses in relation to the used building and insulation materials are also developed. Further, models and tools to allow a technical and economical aggregation, and prediction of energy flexibility from heat pumps and storages that can be used to set up local energy market-places for boosting local renewable resources and cheaper energy prices for the citizens in the local communities are set up. The present deliverable is the outcome of the Task 2.2.

The schematic diagram of the heat pump along with phase change material (PCM) based storage tank is shown in Figure 1.

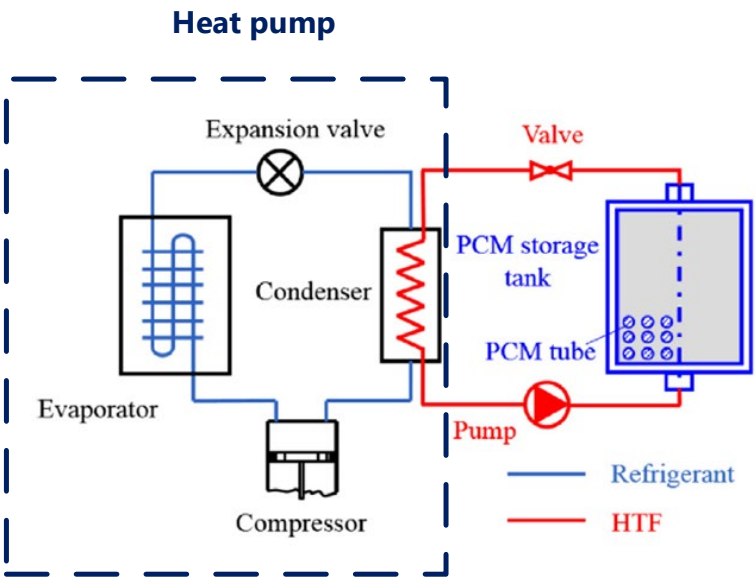

Figure 1: Schematic diagram of HP along with PCM based storage tank system. [1]

The main components being a PCM based storage tank and an air-source heat pump (consisting of a compressor, a condenser and an evaporator) with two key performance indices being charging completion time and total energy usage, both are affected by outdoor temperature and cycling water flow rate. In the heat generation system, electricity is needed for both heat pump and water pump. The charging process associated with PCM technology is non-linear unlike sensible heat technology. The heat pump collects heat from the ambient air,

transferring the heat to cycling water, which in turn delivers heat to the storage tank, where the heat transfer fluid (HTF) is water. The temperature of the PCM increases quickly before phase change but changes slowly during phase change. The coefficient of performance (COP) and power to the heat pump changes significantly due to the dynamic operation with latent heat technology. The important issue concerning the dynamic behavior of PCM is its charging speed, which depends on the thermal properties of the PC materials and configuration of storage tank [2]. The simulation study model is shown in Figure 2. It shows the PCM model from Matlab interfaced with HP model from DIgSILENT, where final model is simulated in DIgSILENT.

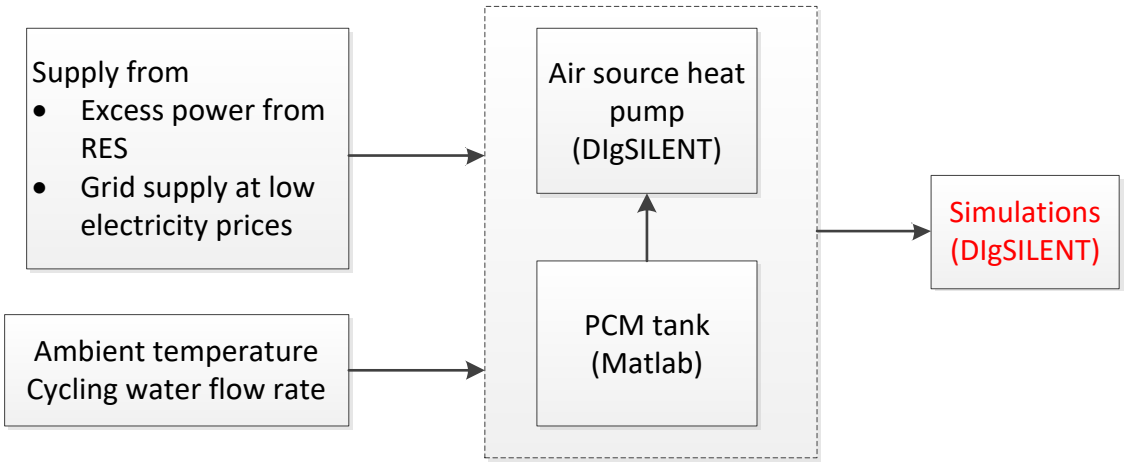

Figure 2: Simulation study model

The input energy to heat pump is supposed to derive from excess generation from renewable energy sources and also from the main grid when the grid electricity prices are low. The model of the Heat Pump (HP) is developed in DIgSILENT and PCM based hot water storage tank (HWST) is developed in Matlab and interfaced with DIgSILENT and is shown in Figure 3. It contains heat pump, PCM based storage tank that is interfaced with Matlab, and Solar-PV is considered for renewable generation. The detailed modeling is described in the following sections.

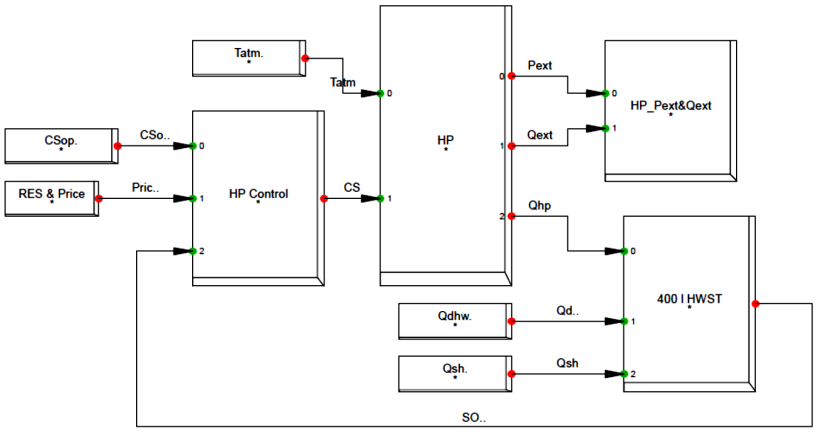

Figure 3: DIgSILENT model of Heat pump and PCM based storage tank

Heat pump model

The heat pumps are rated at P_{HP}=6 & 7 kW with a power factor of 0.98 lagging. Assuming that a constant speed compressor drives the unit, a soft starter is modelled based on [3]. This should limit the starting current to two times its nominal a second after it is turned ON. Then the thermal power produced by the HP (q_{HP}) is calculated as:

$$q_{HP} = P_{HP} * COP * C_s \quad \text{where, } P_{HP} = P_{HP}^{rt}; \quad C_s \in \{0,1\} \tag{1}$$

The coefficient of performance (COP) is dependent on ambient temperature, C_s is the control signal defining the activation of heat pump according to RES generation availability and low grid electricity prices. Nevertheless, the steady state condition of q_{HP} can only be achieved after 15 minutes for the above-mentioned dynamical system [4]. Taking this into consideration, the energy provided by HP (E_{HP}) is then estimated as:

$$E_{HP} = \frac{1}{3600} * \int q_{HP}\ dt \tag{2}$$

As with electric water heaters, the HP is controlled based on a regular hysteresis control. The unit turns on (C_s=1) when supply drops to lower cut-off band, and the HP will supply the storage tank with thermal energy until the higher band is reached. The heat pump should be ON-OFF control in order to maintain a minimum temperature level within the tank to avoid bacteria growth inside the tanks when temperature falls below certain temperature. This is modeled in DIgSILENT software. The heat pump parameters are as given in the Table I.

Table I: Heat pump parameters

Parameters	**Values**
Power rating P_{HP}	6,7 kW
Storage tank volume V	300 l, 400l
Cos(phi)	0.98
Height	1.475 m
HWST energy capacities	5,7,10,12,15 kWh

PCM based heat storage tank model

Salt hydrates are used as phase change material (PCM) in two different shapes, bullets and sticks. The physical arrangement is as shown in Figure 4 (a) & (b), where sticks and bullets shaped PCM are present in the tanks with water as heat transfer fluid (HTF). The heat storage in the form of latent heat can be effectively achieved by means of phase change materials (salt hydrates in this case), i.e. materials characterized by high latent heat of fusion, which through solidification and melting are able to store and release heat, respectively.

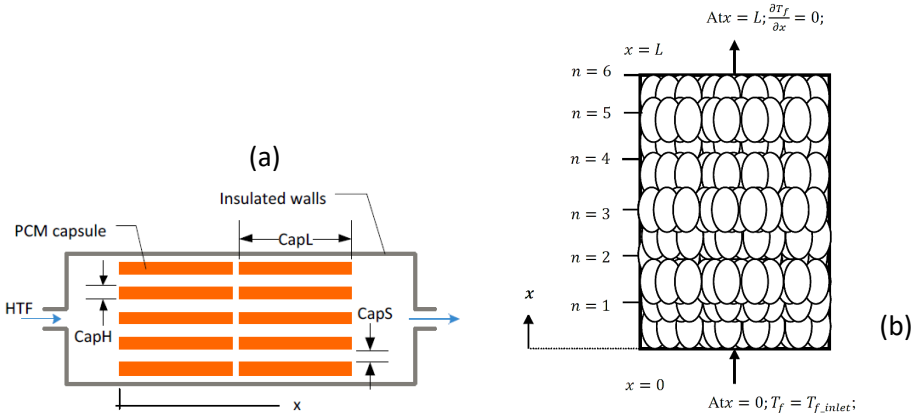

Figure 4 Physical arrangement of model with PCM in two shapes, rectangular sticks (a) and bullets (b).

At time t>0, heat transfer fluid (HTF) i.e., water in current study, flows into the tank at constant temperature. During charging and discharging processes, PCM undergoes three different regimes, which are sensible heating below phase change temperature, phase changes process and sensible heating above phase change temperature. The maximum velocity 'v_{max}' is calculated from the flow rate of HTF across the PCM.

A simplified one-dimensional model is introduced to determine numerically the temperature distribution of the PCM and HTF as well as the location of solid-liquid interface during charging and discharging process. The following assumptions have been made for the model:

a) HTF and PCM are two different domains and have separate equations for each domain region.
b) The thermo physical properties of PCM are different for solid and liquid phases. The variation of properties with respect to temperature during phase change is considered to be linear.
c) The inlet temperature of HTF is constant during the entire charging and discharging processes.
d) The initial temperatures of HTF and PCM are uniform.
e) The resistance offered by the thin wall of capsule is neglected.
f) Radiant heat transfer is neglected.
g) The tank is perfectly insulated.
h) Heat loss from tank surface to the surrounding is neglected

Heat transfer fluid

The temperature of HTF evolves as it flows between PCM capsules and exchanges energy with the capsule wall. For each control volume considered, the energy balance results in the following equation [3],

$$\frac{dC_f T_f}{dt} = \dot{m} c_{pf} \left(T_{in} - T_{out}\right) + h_f A_f \left(T_w - T_f\right) \tag{3}$$

Where, C_f is the HTF heat capacity, m is the mass flow rate of HTF, c_{pf} is the HTF specific heat capacity at a constant pressure, h_f is the heat transfer coefficient between PCM wall and HTF, A_f is the convective surface area. The energy transferred is dependent on the difference between wall temperature T_w and fluid temperature T_f for the control volume.

Using backward time differentiation to solve the for the net rate of energy stored in the HTF control volume, the flow temperature is derived [3] as given in Equation (4),

$$T_f = \frac{(a-b-c)*T_{f0} + c*(T^0_{f(i-1)} + T_{f(i-1)}) + b*(T^0_w + T_w)}{a+b+c}$$
$$a = \rho_f * c_{pf} * V * \Delta t$$
$$b = \frac{h_f * A_f}{2} \quad (4)$$
$$c = \frac{\dot{m} * c_{pf}}{2}$$

where, ρ_f is the HTF density, V is the volume of tank, A_f is the surface area of convective exchange.

Heat transfer to PCM capsule

As the thermal inertia of the capsule wall is neglected, all the energy from HTF is transferred to the wall, q_{conv}, which is transferred to PCM through conduction [3].

$$T_w = \frac{b*(T^0_f + T_f) - (b+d)*T^0_w + d*(T_{PCM} + T^0_{PCM})}{b+d}$$
$$d = \frac{k_{PCM} * A_{PCM}}{\Delta y * 2} \quad (5)$$

where, k_{PCM} is the thermal conductivity of the PCM, A_f is the surface area of conduction exchange and Δy is the conduction distance.

Phase change

During phase change, both the liquid and solid phases are present and are separated by an interface that is constantly shifting. Thus, following the determination of the HTF and capsule wall temperatures, the change in the PCM state is then determined by calculating the change in enthalpy with the equation (6),

$$H = H_0 + q_{conv} * \Delta t$$
$$q_{conv} = h_f * A_f * \left(\frac{T^0_f + T_f}{2} - \frac{T^0_w + T_w}{2} \right) \quad (6)$$

Where H is the current PCM enthalpy, H_0 is the enthalpy of same node for previous time step.

PCM properties

Though PCM conductivity k_{PCM} is assumed constant within one phase, it will vary according to PCM state. It can be determined by the following equation (7) [3],

$$k_{PCM} = k_s + \frac{(H - H_{sm})*(k_l - k_s)}{(H_{sf} - H_{sm})} \quad (7)$$

Where k_s, k_l are the thermal conductivity during solid and liquid states, H_{sf}, H_{sm} are the enthalpy during start of freezing and melting processes. The PCM properties that are chosen are shown in Table II [4].

Table II: PCM properties

Properties	**Solid**	**Liquid**
Specific heat [kJ/kg-°C]	4.226	1.762
Density [kg/m3]	1000	1000
Thermal conductivity [W/m-°C]	0.556	2.22
Latent heat of fusion [kJ/kg]	338	
Melting temperature °C	58	
Initial temperature	80	

Solar-PV model

The power input for the heat pump is extracted from the excess energy from the renewable generation sources (RES) such as solar and wind both at household and community level. In addition, grid energy is used when the electricity prices are low. For the present work, solar-PV is considered and modeled in DIgSILENT, and the respective model is as follows: The active power output of a single PV system, i.e. an array of panels connected to the grid through a single inverter is calculated based on irradiance input data given in the following equation [5],

$$P_{panel} = \frac{E_{g,pv} * E_{pk,panel} * \eta_{rel} * \eta_{inv}}{E_{STD}} \qquad (8)$$

$$P_{system} = P_{panel} * n_{panel}$$

Where,

- P_{panel} is the active power output of the panel in kW
- P_{system} is the single system active power output in kW
- num_{panels} is the number of panels per inverter
- $E_{g;pv}$ is the global irradiance on the plane of the array in W/m^2
- E_{STD} is the standard irradiance value of 1000 W/m^2
- $P_{pk;panel}$ is the total rated peak power of the solar panel in kW
- η_{rel} is the relative efficiency of the panel, unit-less.
- η_{inv} is the efficiency factor of the inverter, unit-less

The installation capacities of solar-PV can be assumed to domestic installations. Using solar irradiance data and solar installation data, the output production can be calculated using Equation (8).

Thermal demand consumption

The total thermal demand consumption profiles for 20 households that are selected for the demonstration-II, where a booster heat hump is to be installed, are as shown in Figure 5. It can be observed from the thermal demand profile, in the first part and last part of the year, the thermal demand is highly varying, and it is low in the summer months of Jun, Jul and Aug, which is understandable.

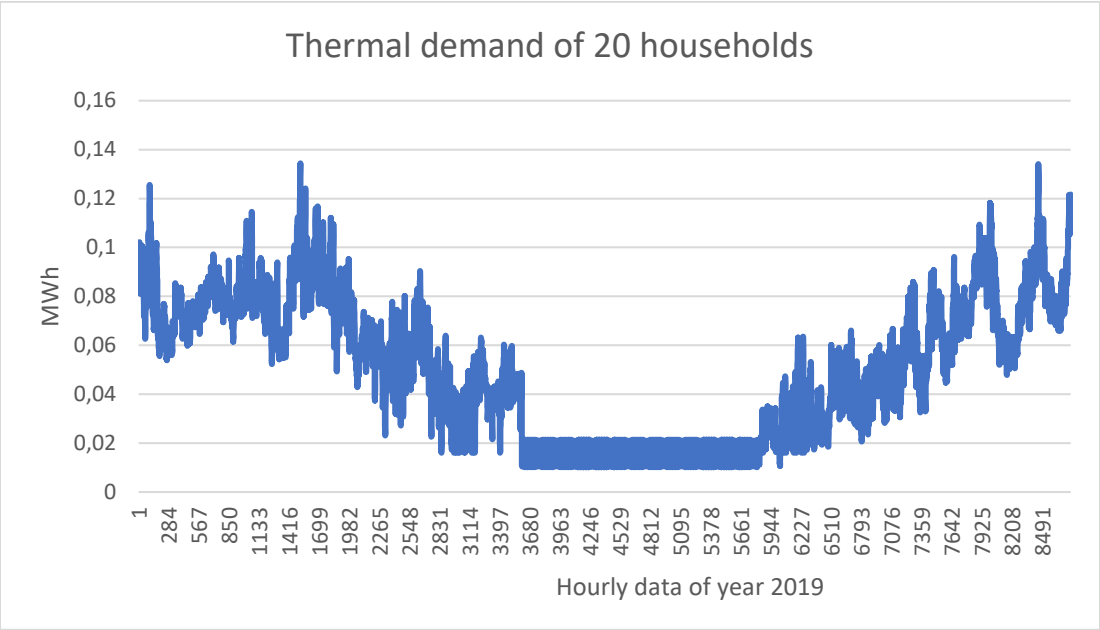

Figure 5: Thermal demand profiles of 20 dwellings

The daily variation for a winter month and summer month is shown in Figs. 6, 7. The average demand on a winter day is 0.0787 MWh and for a summer day is 0.0157 MWh. The Solar-PV production is generally higher during summer months than the winter months, whereas the thermal demand is high in winter months.

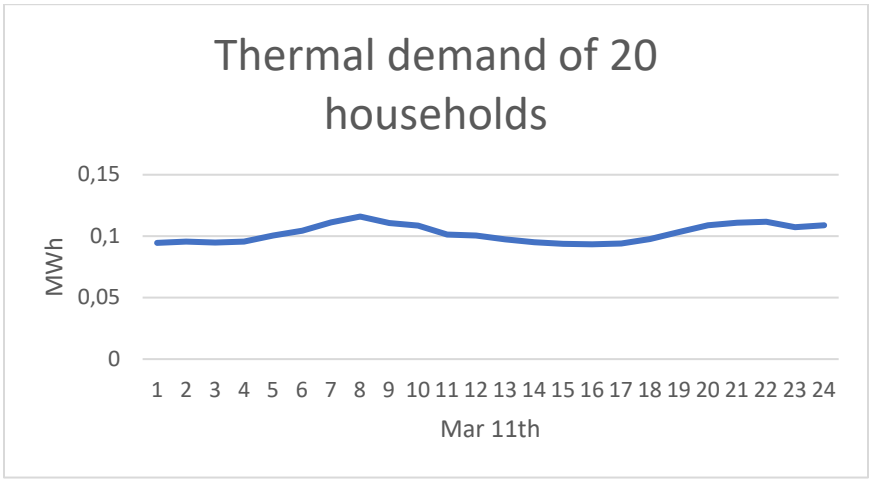

Figure 6: Thermal demand profile for 20 dwellings on a winter day

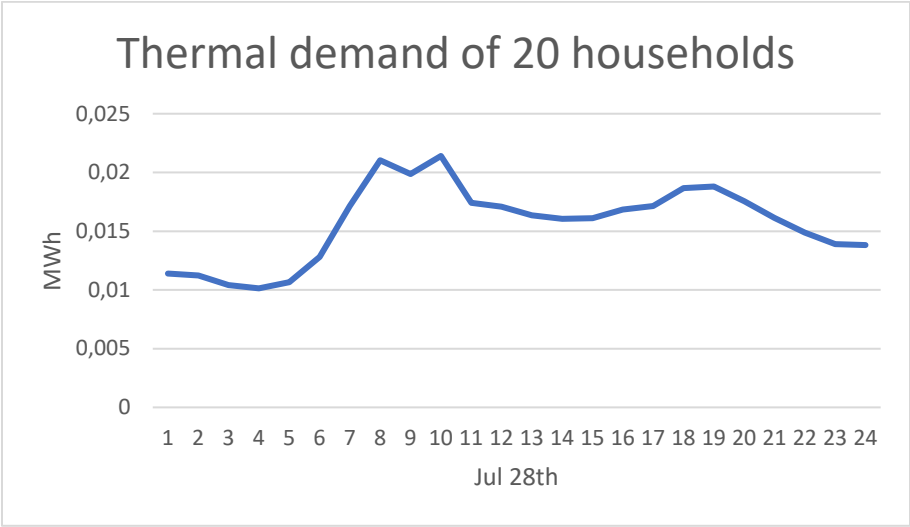

Figure 7: Thermal demand profile for 20 dwellings on a summer day

The Elspot prices from Energinet's data hub for the year 2019 is as shown in Figure 8. It can be observed that the spot prices are highest in the month of January and went to negative several times durins the month of March. Further from Fig. 5 (data points 1416-2160), it can be clear that the month of March witnessed high thermal demand. Considering this, March month would be a good business case, where electricity price is at its low and it is benefitting to use the locally generated RES production for meeting most of the thermal demand.

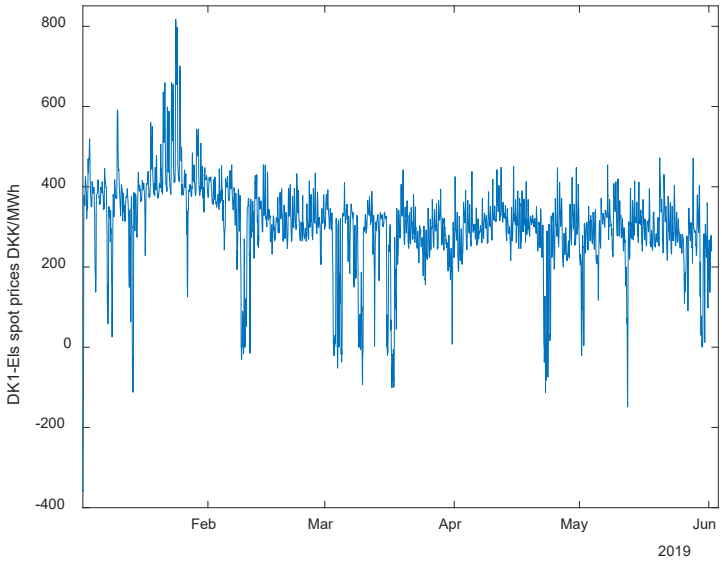

Figure 8: Elspot prices of DK1

Control algorithms

The HP's will be intelligently operated whenever there is excess renewable energy sources (RES) including Solar-PV or Wind units, located either within households or within local community. Accordingly, the control algorithms are derived for the two demonstration sites.

Demonstration site- I

The key deciding factors in the intelligent scheduling of HP's in Demo-1 are:

- Consumer's comfort and preferences,
- Electricity prices,
- Finally, the distribution network limits.

The output from the optimization will be a trade-off among the above three main constraints. The motivation is to benefit consumer in both the use-cases.

Use case-I.A (optimizing the utilization of renewable production at household level)

Optimizes each household's HP operation along with its storage by the **excess renewable energy from that household** through electricity to heat system within the household.

Use case-I.B (optimizing the utilization of renewable production at community level)

Optimizes each household's HP operation along with its storage by the **excess renewable energy from local community** by electricity to heat system in the household.

Control algorithm for Demo-I

Once the prediction of overproduction from renewables at either household or aggregated level is available then,

- The objective is to reduce the cost of importing energy from the grid by efficiently utilizing the renewables), if RES is at household level, or increasing the renewable integration in the grid, if RES is at aggregated level, by using electricity to heat network systems.
- The local controller associated with HP's at consumer site provides the state of HP and energy level within storage tank, to the central controller (PreHEAT Aggregator).
- The central controller gathers the information about over production, electricity price along with consumer preference as the main constraints to determine the optimal operation of HPs.

In addition, the electrical network constraints, such as voltage limits, would also be considered as one of the constraints.

For 1A (Optimization for household h):

$$\text{Min} \sum_{t} \left[H_{ED}(\text{h,t}) - H_{GEN}(\text{h,t}) \right] \times Elspot(t) + \left[DCF_{TD}(h,t) \times \text{Pr}\, ice_{DCF}(t) \right] \quad (9)$$

For 1B (Optimization for community level):

$$\text{Min} \sum_{t} \left[\sum_{h} \left[H_{ED}(\text{h,t}) - H_{GEN}(\text{h,t}) \right] \times Elspot(t) + \left[DCF_{TD}(h,t) \times \text{Pr}\, ice_{DCF}(t) \right] \right]$$

Constraints (for both 1A and 1B),

$\forall$t:

$$\sum_{h}\left[ED(h,t)-P_{RES}(h,t)\right]\leq feedercapacity(t)$$

$$U_{\min}\leq Voltage_{area}(t)\leq U_{\max}$$

and $\forall h,\forall t$:

$$Q_{\min}(h,t)\leq \text{householdtank}_{SOE}(h,t)\leq Q_{\max}(h,t)$$

$$C_{\min}(h,t)\leq comfort(h,t)\leq C_{\max}(h,t)$$

$$H_{Gen}=H_{PV}+H_{\text{Im}port}$$

$$if\ H_{PV}=0,\ \text{then import from grid}$$

where,

DCF_{TD} is the discomfort demand

Price_{DCF} is the price for discomfort

ED is the electrical demand towards HP

P_{RES} is the excess power from RES

(10)

Demonstration site-II

Booster heat-pump station setup

The objective is to supply heating at required temperature level to specific area using booster HP along with its storage tank by utilizing and boosting the return temperature from DH network in another area. The sizing of the booster heat pump was carried out by Neogrid and Suntherm, based upon historical consumption data for the area provided by Skive Fjernvarme.

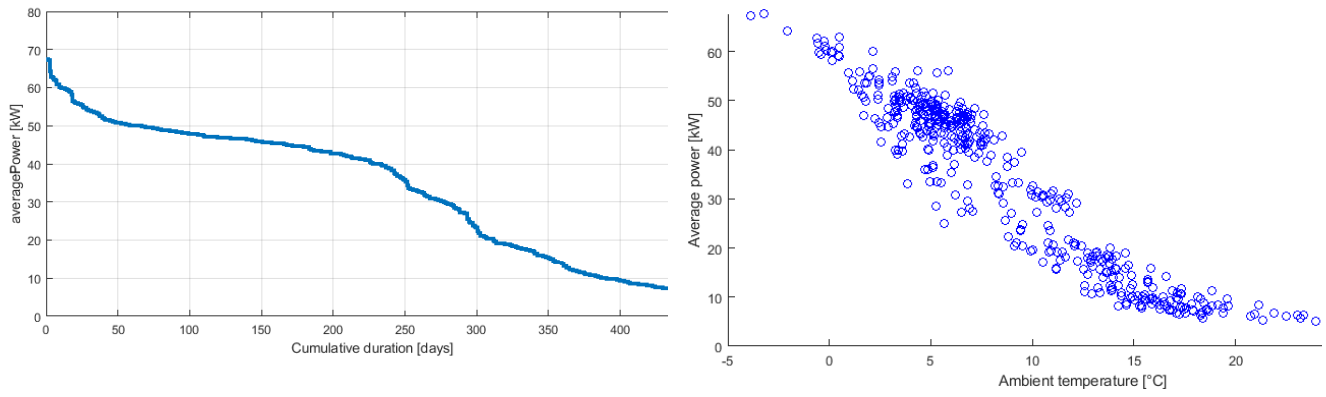

Figure 9: Duration curve for the average daily load in the area and dependency of the total load in the area to the ambient temperature (daily data)

The booster heat-pump station includes the following elements:

- On primary side of the heat-pump: a buffer water tank on its primary side (to compensate for flow fluctuations in the return line that is used)
- On the secondary side of the heat-pump: a PCM tank, and then a heat-exchanger to the local area (to avoid getting district heating water into the PCM tank)

This setup is illustrated on the figure below:

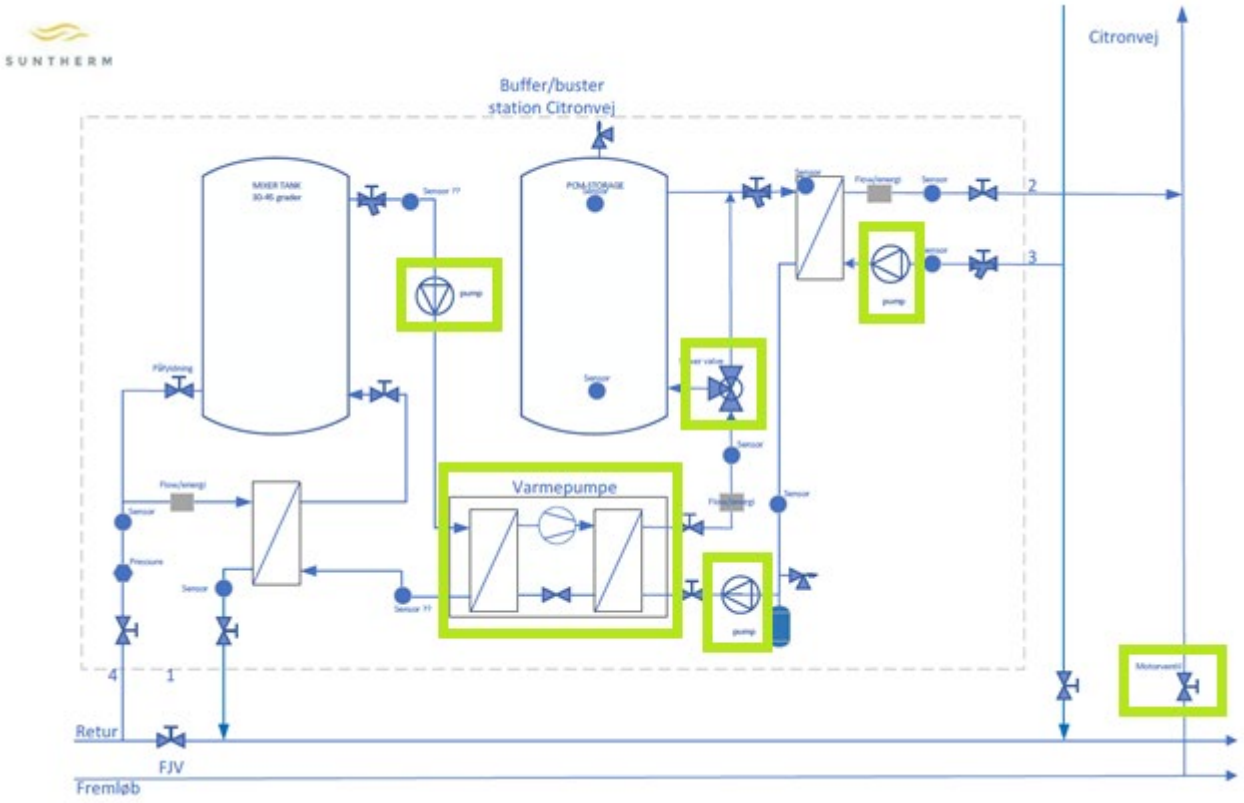

Figure 10: System layout for the booster station and connection to the area (green blocks indicate actuators to be controlled)

In terms of controls, an online controller will optimise the operation of the following actuators:

- Pump (flow) on the primary side of the heat-pump
- Start/Stop of heat-pump and level of operation (0, 50, 100%)
- Pump (flow) on secondary side of the heat-pump
- 3-point valve from the heat-pump to the PCM tank and/or exchanger
- Pump (flow) to the local area
- A back-up valve to the local district heating (not meant to be used in normal operation, but allowing a fast switch back in case of a failure in the experimental booster)

Control of the booster heat-pump station

The operation of the heat-pump and its PCM tank is optimized to minimize the cost of operation of the booster heat pump.

This optimization is carried out within constraints of voltage and feeder capacity (for the electrical part), and supply temperature delivered to the area (for the district heating part, which implicitly includes comfort constraints in the individual houses)

- Consumer preferences and electrical network operating limits will form the constraints.
- The storage tank associated with booster HP,
    - Charges when there is either excess production from RES or low electricity prices.
    - Discharges whenever there is a need to level the flow temperature of the selected area's DH network.

Formally, this would result in the following optimization programs (where *t* designates time, and *h* designates a particular household):

$$min_{t \in T_{window}} \; Booster_{ED}(t) \times (Elspot(t) \; + penalties(t)) \tag{11}$$

Under constraints, for all $t \in T_{window}$:

$$Booster_{ED}(t) - Local_{GEN}(h,t) + \sum_{h} Local_{ED}(h,t) \; \leq Feeder\ capacity(t)$$

$$U_{min} \leq Voltage_{area} \leq U_{max}$$

$$T_{supply,min}(t) \leq T_{supply,area}(t) \leq T_{supply,max}(t)$$

$$Q_{min} \leq SOE_{PCM\ tank} \leq Q_{max}$$

$$\sum_{h} Heat\ demand\ (h,t) + area\ heat\ loss(t) \; \leq Booster\ station\ capacity(t)$$

And for all households h:

$$Indoor\ temperature(h,t) \geq minimum\ temperature(h,t)$$

$$Hot\ water\ temperature(h,t) \geq minimum\ hot\ water\ temperature(h,t)$$

Where the cost of electricity contains the spot price (*Elspot* term) as well as other charges/levies (network tariffs, emissions, taxes, … - modelled in the *penalties* term).

Simulations results:

This section shows the simulations results of working models of heat pump and PCM based tank. The differential equations (3)-(7) are solved using ODE solvers from Matlab to determine the operation of PCM for both cooling and heating conditions. The PCM properties from Table II are considered for the current simulations.

PCM model output: With and without energy input

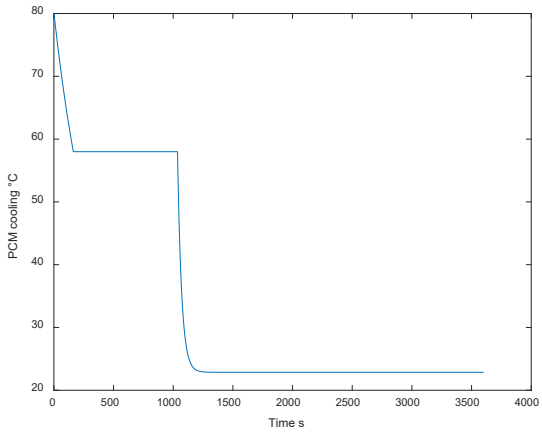

Figure 11: PCM cooling temperature with no energy inputs

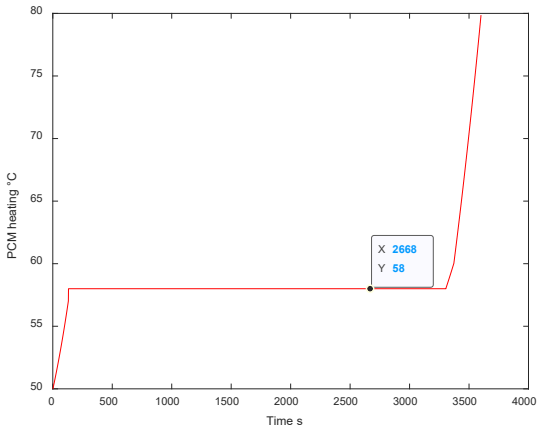

Figure 12: PCM heating temperature with energy inputs from HP

The temperature profiles of PCM when cooling and heating are as shown in Figs. 11 &12. Fig. 11 show the temperature profile of PCM where the current energy in the storage tank sets the temperature to 80 ^{0}C and there is no external energy input from HP. It can be observed that the temperature begins to decrease due to withdrawal of energy from the tank and it follows a linear curve until it reaches freezing temperature. At this point the temperature remains constant as the PCM solidifies. The freezing temperature is 58 ^{0}C, which is provided by Suntherm partners. The transition of PCM liquid state to solid is rather sudden, whereas the transition of further decreasing in the temperature is more gradual. The temperature of the PCM continues to decrease until it reached the ambient temperature. Fig. 12 shows the temperature profile of PCM, while there is a constant input flow at 35 ^{0}C from HP and no demand. It can be observed that there is fast and clear increase in temperature during solid phase. This differs from cooling curve by not experiencing long prolonged phase change period. Figs. 13, 14 show the state of energy (SOE) of the HWST without and with demand from floor heating and domestic hot water, respectively. Whenever the temperature inside the tank becomes greater than melting temperature i.e., 58 degrees centigrade of PCM, the PCM melts and the energy releases, which can be used for meeting the thermal demand. It can be observed from Fig. 14, the HP switches ON many times in a day in order to meet the thermal demand. This switching pattern varies with respect to excess RES input, low electricity prices from grid and consumers' comfort.

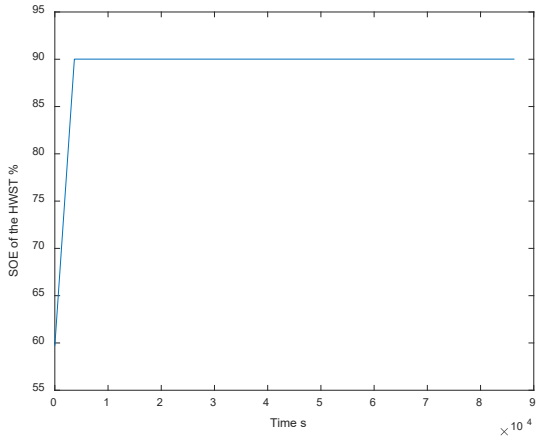

Figure 13: A 24-hour SOE profile of HWST with no demand

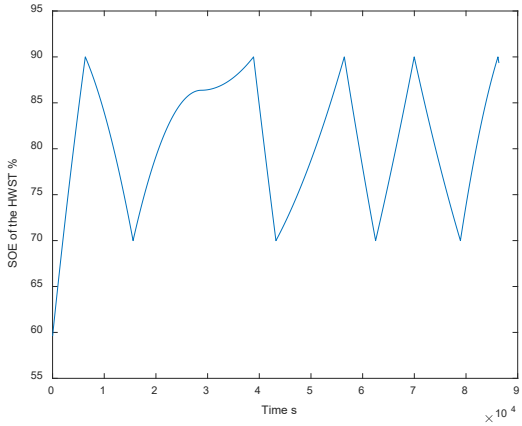

Figure 14: A 24-hour SOE profile of HWST with thermal demand

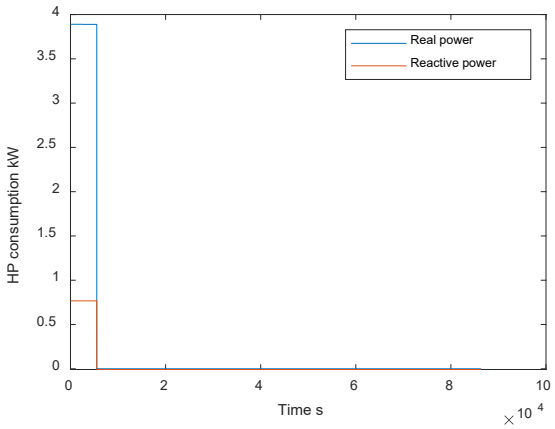

Figure 15: Real and reactive power consumption of HP when no demand

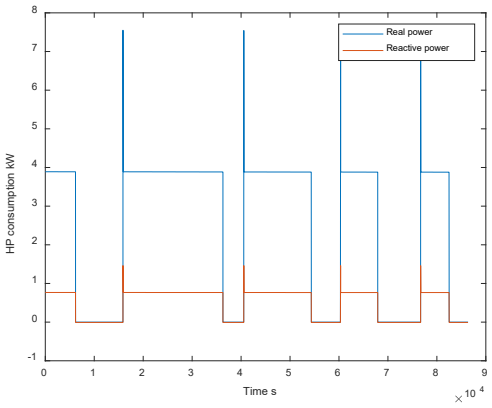

Figure 16: Real and reactive power consumption of HP with demand

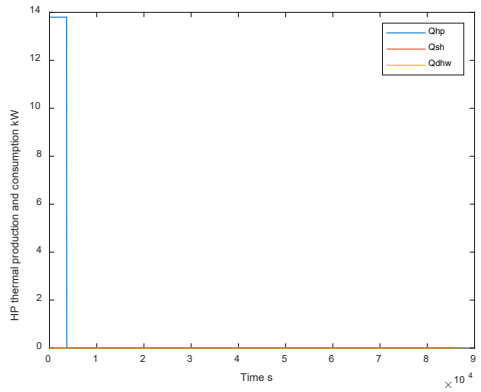

Figure 17: Thermal production and consumption of HP when no demand

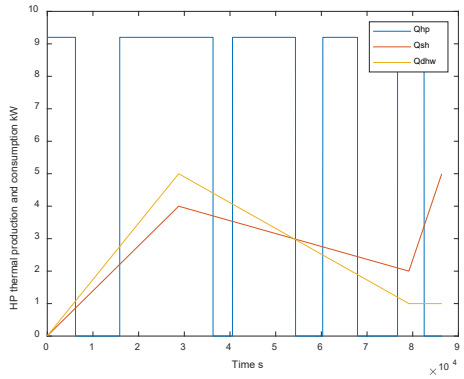

Figure 18: Thermal production and consumption of HP with demand

The real and reactive power consumption profiles of HP without and with demand are as shown in Figs. 15 & 16. At the beginning of the simulation, the control signal is given as C_s=1, which means ON signal, so the HP is ON but with time as thermal demand is increasing HP remained in ON position till the tank energy reaches upper

hysteresis band. Figs. 17 & 18 show the thermal energy production and consumption profiles of HP. The demand profiles for space heating and hot water are assumed values. The hysteresis band considered for HP is between 70 % and 90% of state of energy (SOE) of the tank. It can be observed from Figs. 14 & 16, whenever SOE of tank reaches 70% of energy, the HP switches ON till SOE reached 90%. In the current simulation studies, the ON-OFF control of HP operation is considered. The results till now are showing the operation of HP with PCM based storage tank without and with demand. The rest of the results are shown for the intelligent operation of HP for maximizing the renewable energy penetration towards meeting thermal demand of the selected houses from Skive commune. The base case scenario is where the total thermal demand is met by the grid electricity and the considered electricity spot prices [6] are shown in Fig. 19. The thermal consumption for a typical day with high thermal demand is as shown in Figs. 6. In addition, the estimated production from solar PV installation at households is shown in Fig 19. It is assumed that each household is having 5 kW Solar-PV installations.

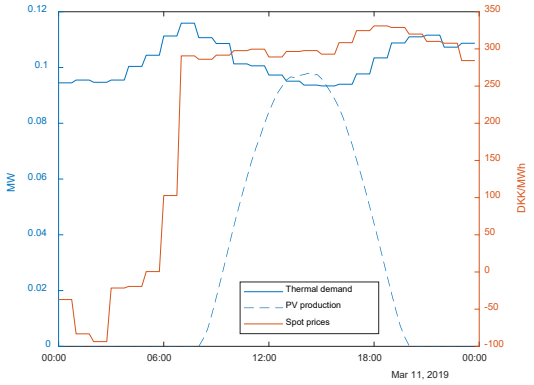

Figure 19: On-site estimated Solar-PV production, given thermal demand for 20 households and Elspot prices [6]

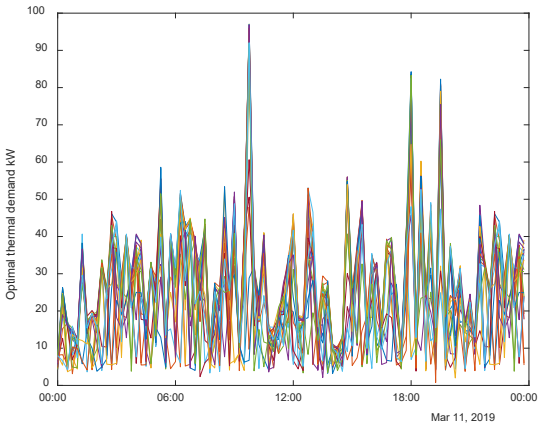

Figure 20: Proposed optimal thermal demand profiles

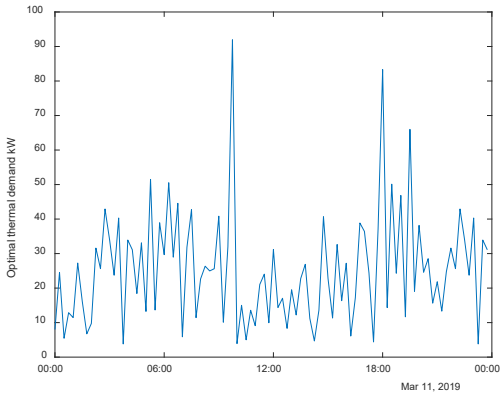

Figure 21: Optimal demand profile for one household during RES production period

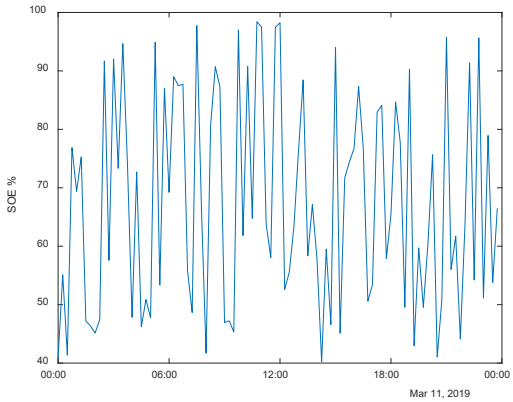

Figure 22: SOE percentage in the storage tank to the optimal demand shown in Fig 22.

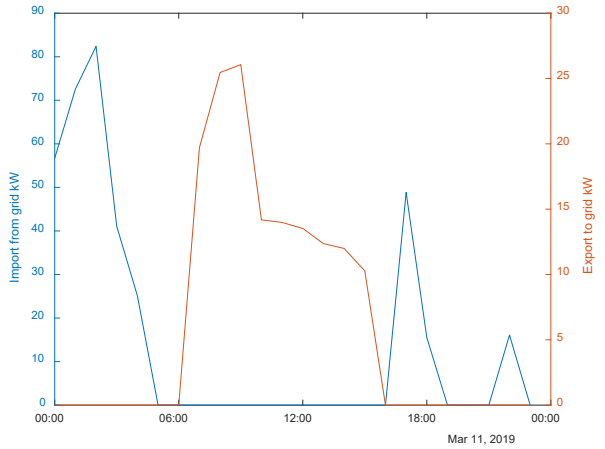

Figure 23: Import/Export of power with respect to the grid.

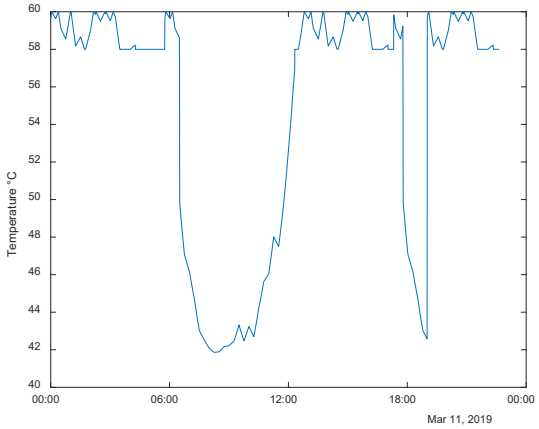

Figure 24: Temperature inside storage tank for one household

Table III Electricity payment without and with intelligent HP control for a day with hourly data (for all 20 households)

Without HP control	With HP control
388.68 DKK	262.93 DKK

Without and with the intelligent operation of HP, the results are shown in Table III. It is to be observed that the thermal demand is high during the period where the generation from RES is low. According to the proposed optimization model from Equation (9) & (10), the HP operates during low electricity price period and fully charge the storage tank. It tries to meet the thermal demand with the charged tank. This kind of operation is beneficial for three stake holders including the consumer, aggregator and system operator. Solving the optimization problem given in the equations (9) and (10) using genetic algorithm, the optimal demand profile for all the households is as shown in Figure 20. Comparing the optimal demand with Fig. 20, the original thermal demand profile has observed peaks during morning and late evening, where there is no Solar-PV production available. Whereas, the optimal demand is having observed peaks during Solar-PV production period and also in the late evening. Indirectly there is little inconvenience caused to the consumer when maximizing consumption during production periods. Figure 23 shows the overall import from grid and export to grid with respect to all the 20 households. It can be observed there is less export to the grid during solar-PV production period i.e., 9 am – 5 pm and import from the grid is taken place whenever there are negative electricity prices along with the periods when thermal demand could not met by the available energy in the tanks. It is to be noted from Fig 24, the tank is being charged during mid-night as the electricity price is negative and also during mid-afternoon due to availability of the local solar-PV production. Figs. 22 and 24 show the SOE and temperature levels in the storage tank. The temperature inside the tank is maintained between ranges of 40 – 60 degrees and can be observed from Fig 24 that the temperature is reaching the minimum range due to thermal demand peaks during morning and late evening. It is attempted to maintain the SOE at minimum 40 % limit and it can be observed that the SOE of the tank is going low during morning between 9 am – 10 am and also in the late evening between 6 pm – 7pm, due to the fact that there is peak in thermal demand as seen from Fig. 19. Further, the storage is being charged because of the on-site solar-PV production at the households during 9am – 5 pm, as can be observed from Fig. 22. The

objective function value is the electricity price paid by the consumer without and with HP control and this result is given in Table III, which is evident that the payment by the consumer towards meeting thermal demand has considerable reduced when compared to the case without intelligent control of HP. The inconvenience created for the consumer (in terms of shifting demand with respect to production periods) is given as cost to be paid by aggregator, this is not considered in these simulations but later can be added.

Installations used in the demonstrations

In demonstration I, with heat-pumps in individual houses:

- The 31 houses have a heat-pump with a rated capacity of 6-9 kW, and a tank with a volume of 300-400 L. Out of these, 9 houses have PCM materials in their tank while the rest has only water as a heat buffer in their tank.
- Maximum daily heat demand varying within 45-175 kWh
- 6 houses have local PV production, and 2 of them have solar thermal production

In demonstration II, with booster heat-pumps and substation control in individual houses:

- The 20 houses have a maximum daily heat demand varying within 58-118 kWh.
- There is little local energy production, with only 2 houses having installed PV panels (though this is irrelevant to the optimization of this use-case).

Price and emission data for electricity are loaded from Energinet's Datahub.

Summary

The deliverable reported the working models of the heat pump with PCM based storage tank and solar-PV model. Comparing the thermal demand profiles and Elspot prices, it is said that the March month can provide a good business case for effective demonstration of the control algorithms. Further, the control algorithms of the heat pump for both the demonstration sites that are derived from Task 2.1 are used here and simulated. The optimization equations are formulated by the Neogrid partners. This report also presented the simulation studies for the operation of HP with PCM based storage tank with and without thermal demand. In addition, the HP control algorithm that is proposed for Demonstration-I is tested for a given thermal demand, renewable production and electricity spot prices and the results are explained. Validating the simulation results with both demonstration sites will be part of Task 2.3 with next deliverable in M26.

References

[1] Yantong Li, Nan Zhang, Zhixiong Ding, ''Investigation on the energy performance of using air-source heat pump to charge PCM storage tank,'' *Journal of Energy Storage*, Vol. 28, pp. 1-15, Apr. 2020.

[2]. Y. Tao, Y. Liu, Y.-L. He, ''Effects of PCM arrangement and natural convection on charging and discharging performance of shell-and-tube LHS unit,'' Int. J. Heat Mass Transf., 115, pp. 99–107, 2017.

[2] M. Akmal, B. Fox, D. Morrow, and T. Littler, "Impact of high penetration of heat pumps on low voltage distribution networks," in PowerTech, 2011 IEEE Trondheim, June 2011, pp. 1–7.

[3] T. Masuta, A. Yokoyama, and Y. Tada, “Modeling of a number of Heat Pump Water Heaters as control equipment for load frequency control in power systems,” in IEEE Trondheim PowerTech, , June 2011, pp. 1–7.

[4] N. K. Bansal, and D. Buddhi, ‘‘An analytical study of a latent heat storage system in a cylinder,’’ Journal of energy conversion and management, vol. 33, pp. 235-242, 1992.

[5]. D’Avignon, K., and M. Kummert. 2012. “Proposed TRNSYS Model for Storage Tank with Encapsulated Phase Change Materials.” 5th National Conference of IBPSA-USA, Madison, WI, USA.

[6]. DIgSILENT User manual, https://www.digsilent.de/en/downloads.html

[7]. https://www.energidataservice.dk/

[8]. https://www.nordpoolgroup.com/Market-data1/#/nordic/table